

# Quantum Equivalence and Quantum Signatures in Heat Engines

Raam Uzdin, Amikam Levy, and Ronnie Kosloff\*  
*Fritz Haber Research Center for Molecular Dynamics,  
Hebrew University of Jerusalem, Jerusalem 91904, Israel*

Quantum heat engines (QHE) are thermal machines where the working substance is quantum. In the extreme case the working medium can be a single particle or a few level quantum system. The study of QHE has shown a remarkable similarity with the standard thermodynamical models, thus raising the issue what is quantum in quantum thermodynamics. Our main result is thermodynamical equivalence of all engine type in the quantum regime of small action. They have the same power, the same heat, the same efficiency, and they even have the same relaxation rates and relaxation modes. Furthermore, it is shown that QHE have quantum-thermodynamic signature, i.e thermodynamic measurements can confirm the presence of quantum coherence in the device. The coherent work extraction mechanism enables power outputs that greatly exceed the power of stochastic (dephased) engines.

## I. INTRODUCTION

Thermodynamics emerged as a practical theory for evaluating the performance of steam engines. Since then the theory proliferated and utilized in countless systems and applications. Eventually, thermodynamics became one of the pillars of theoretical physics. Amazingly, it survived great scientific revolutions such as quantum mechanics and general relativity. In fact, thermodynamics played a crucial role in the development of these theories. Black body radiation led Planck and Einstein to introduce energy quantization, and the second law of thermodynamics led Bekenstein to discover the relation between the event horizon area and black hole entropy and temperature.

The Carnot efficiency is a manifestation of the second law in heat engines, and it is universally valid. In addition all reversible engines must operate at Carnot efficiency. Though very profound these principles have limited practical value. First, real engines produce finite non zero power and therefore cannot be reversible. Second, the performance of real engine is more severely limited by heat leaks, friction and heat transport. This led to the study of efficiency at maximal power [1, 2] and finite time thermodynamics [3, 4]. In finite time thermodynamics time was introduced classically using empirical heat transport models. For microscopic systems the natural avenue to introduce time dynamics is via quantum

mechanics of open systems. The full quantum dynamics may lead to new mechanism of extracting work or cooling. Alternatively, it may lead to new microscopic heat leaks and friction-like mechanisms.

Quantum thermodynamics is the study of thermodynamic quantities such as temperature, heat, work, and entropy in microscopic quantum systems or even for a single particle. This includes dynamical analysis of engines and refrigerators in the quantum regime [5–27], theoretical frameworks that takes into account single shot events [28, 29], and the study of thermalization mechanisms [30–32].

It was natural to expect that in the quantum regime new thermodynamic effects will surface. However, quantum thermodynamic systems (even with a single particle) show a remarkable similarity to macroscopic system described by classical thermodynamic. When the baths are thermal the Carnot efficiency limit is equally applicable for a small quantum system [5, 33]. Even classical fluctuation theorems hold without any alteration [34–36].

Is there really nothing new and profound in the thermodynamics of small quantum system? In this work, we present thermodynamic behavior that is purely quantum in its essence and has no classical counterpart.

Recently some progress on the role of quantum coherence in quantum thermodynamics has been made [37, 38]. In addition, quantum coherence has been shown to quantitatively affect the performance of heat machines [39–41]. In this work we associate coherence with a specific *thermodynamic effect* and relate it to a *thermodynamic work extraction mechanism*.

Heat engines can be classified by their different scheduling of the interactions with the baths and the work repository. These types include the four-stroke, two-stroke and the continuous engines (these engine types will be described in more detail later on). The choice of engine type is usually guided by convenience of analysis or ease of implementation. Nevertheless, from a theoretical point of view, the fundamental differences or similarities between the various engine types are still uncharted. This is particularly true in the microscopic quantum regime. For brevity we discuss engines but all our results are equally applicable to other heat machines such as refrigerators and heaters.

Our first result is that in the limit of small engine action (weak thermalization, and a weak driving field), all three engine types are thermodynamically equivalent. The equivalence holds also for transients and for states that are very far from thermal equilibrium. On top of providing a thermodynamic unification limit for the various engine types, this finding also establishes a connec-

---

\*Electronic address: raam@mail.huji.ac.il

tion to quantum mechanics as it crucially depends on phase coherence and quantum interference. In particular, the validity regime of the equivalence is expressed in terms of  $\hbar$ .

Our second result concerns quantum-thermodynamic signatures. Let us define a *quantum signature* as a signal extracted from measurements that unambiguously indicates the presence of quantum effects (e.g. entanglement or interference). The Bell inequality for the EPR experiment is a good example. A *quantum-thermodynamic signature* is a quantum signature obtained from measuring thermodynamic quantities. We show that it is possible to set an upper bound on the work output of a stochastic, coherence-free engine. Any engine that surpasses this bound must have some level of coherence. Hence, work exceeding the stochastic bound constitutes a quantum-thermodynamic signature. Furthermore, we distinguish between a coherent work extraction mechanism and a stochastic work extraction mechanism. This explains why in the equivalence regime, coherent engines produce significantly more power compared to the corresponding stochastic engine.

The equivalence derivation is based on three ingredients. First, we introduce a multilevel embedding framework that enables the analysis of all three types of engines in the same physical setup. Next, a “norm action” smallness parameter,  $s$ , is defined for engines using Liouville space. The third ingredient is the symmetric rearrangement theorem that is used to show why all three engine types have the same thermodynamic properties despite the fact that they exhibit very different density matrix dynamics.

In section two we describe the main engine types, and introduce the multilevel embedding framework. Next, in section three the multilevel embedding and the symmetric rearrangement theorem are used to show the various equivalence relation of different engine types. After discussing the two fundamental work extraction mechanisms, in section four we present and study the overthermalization effect in coherent heat engines. In section five we show a quantum thermodynamic signature that separates quantum engines from stochastic engines. Finally, in section six we conclude and discuss extensions and future prospects.

## II. HEAT ENGINES TYPES AND THE MULTILEVEL EMBEDDING SCHEME

Heat engines are either discrete such as the two stroke engines or the four stroke Otto engine. Heat engines can also operate continuously such as in turbines. Quantum analogues of all these engine types have been studied[73]. Here we present a theoretical framework where all three type of engines can be embedded in a unified physical framework. This framework termed “multilevel embedding” is an essential ingredient in our theory as it enables a meaningful comparison between different engine types.

### A. Heat and work

A heat engine is a device that uses at least two thermal baths in different temperatures to extract work. Loosely speaking, work is the transfer of energy to a single degree of freedom. For example, increasing the excitation number of an oscillator, increasing the photon number in a specific optical mode (lasing) or increasing the kinetic energy in a single predefined direction. “Battery” or “flywheel” are terms often used in this context of work storage [42, 43]. We shall use the more general term “work repository”. Heat, on the other hand, is energy spread over multiple degrees of freedom. Close to equilibrium and in quasistatic process, the heat is related to the temperature and to the effective number of degrees of freedom (entropy  $S$ ) via the well known relation  $dQ = TdS$ .

In the elementary quantum heat engines the working substance comprises of a single particle (or few at the most). Thus the working substance cannot reach equilibrium on its own. Furthermore, excluding few non-generic cases it is not possible to assign an equation of state that establishes a relation between thermodynamic quantities when the substance is in equilibrium. Nevertheless, QHE satisfy the second law and therefore are also bounded by Carnot efficiency limit [5].

Work strokes are characterized by zero contact with the baths and an inherently time dependent Hamiltonian. The unitary evolution generated by this Hamiltonian can change the energy of the system. On the other hand, the von Neumann entropy and the purity, remain fixed (unitary evolution at this stage). Hence the energy change of the system in this case constitutes pure work. The system’s energy change is actually an energy exchange with the work repository.

When the system is coupled to a thermal bath and the Hamiltonian is fixed in time, the bath can change the populations of the energy levels. In steady state the system reaches a Gibbs state where the density matrix has no coherences in the energy basis and the population of the levels is given by:  $p_{n,b} = e^{-\frac{E_n}{T_b}} / \sum_{n=1}^N e^{-\frac{E_n}{T_b}}$  where  $N$  is the number of levels and ‘ $b$ ’ stands for ‘ $c$ ’ (cold) or ‘ $h$ ’ (hot). In physical models where the system thermalizes via collision with bath particles a full thermalization can be achieved in finite time [44–48]. However, it is not necessary that the baths will bring the system close to a Gibbs state for the proper operation of the engine. In particular, maximal efficiency (e.g. in Otto engines) can be achieved without full thermalization. Maximal power (work per cycle time) is also associated with partial thermalization [1, 49]. The definitive property of a thermal bath is its aspiration to bring the system to a predefined temperature regardless of the initial state of the system. The evolution in this stage does not conserve the eigenvalues of the density matrix of the system, and therefore not only energy but entropy as well is exchanged with the bath. Therefore, the energy exchange in this stage is considered as heat.

In contrast to definitions of heat and work that are based on the derivative of the internal energy [5, 50, 51], our definitions are obtained by energy balance when coupling only one element (bath or external field) at a time. As we shall see later on, in some engine types several agents change the internal energy simultaneously. Even in this case, this point of view of heat and work will still be useful for obtaining consistent and physical definitions of heat and work.

## B. The three engine types

There are three core engine types that operate with two thermal baths: four-stroke engine, two-stroke engine, and a continuous engine. A stroke is a time segment where a certain operation takes place, for example thermalization or work extraction. Each stroke is a  $CP$  map and therefore the one-cycle evolution operator of the engine is also a  $CP$  map (since it is a product of  $CP$  maps). For the extraction of work it is imperative that some of the stroke propagators do not commute [52].

Otto engines and Carnot engines are examples of four stroke engines. The simplest quantum four-stroke engine is the two-level Otto engine shown in Fig. 1a. In the first stroke only the cold bath is connected. Thus, the internal energy changes are associated with heat exchange with the cold bath. The expansion and compression of the levels are fully described by a time-dependent Hamiltonian of the form  $H(t) = f(t)\sigma_z$  (the baths are disconnected at this stage). In the second stroke, work is consumed in order to expand the levels, and in the fourth stroke work is produced when levels revert to their original values. There is a net work extraction since the populations in stages II and IV are different. As we shall see later on, other unitary operations are more relevant for quantum equivalence of heat engines. Nevertheless, this particular operation resembles the classical expansion and compression of classical engines. The work is the energy exchanged with the system during the unitary stages:  $W = W_{II} + W_{IV} = (\langle E_3 \rangle - \langle E_2 \rangle) + (\langle E_5 \rangle - \langle E_4 \rangle)$ . We will consider only energy expectation values for two main reasons. First, investigations of work fluctuations revealed that quantum heat engines follow classical fluctuation laws [53] and we search for quantum signatures in heat engines. The second reason is that in our view the engine should not be measured during operation. The measurement protocol used in quantum fluctuation theorems [34, 35, 53], eliminates the density matrix coherences. These coherences have a critical component in the equivalence and quantum signature we study in this paper. Thus, although we frequently calculate work per cycle, the measured quantity is the cumulative work and it is measured only at the end of the process. The averaged quantities are obtained by repeating the full experiment many times. Engines are designed to perform a task and we assume that this completed task is the subject of measurement. The engine internal state are not

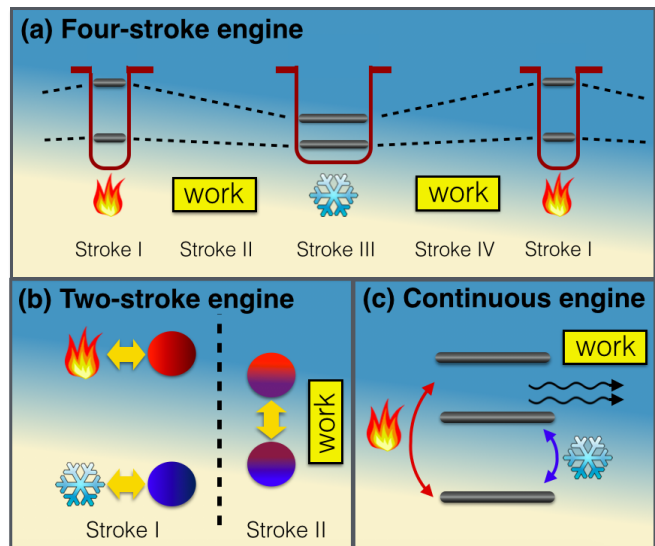


Figure 1: (a) A two-level scheme of a four-stroke engine. (b) Two-particle scheme of a two stroke engine. (c) A three-level scheme of a continuous engine.

measured.

The heat per cycle taken from the cold bath is  $Q_c = \langle E_2 \rangle - \langle E_1 \rangle$  and the heat taken from the hot bath is  $Q_h = \langle E_4 \rangle - \langle E_3 \rangle$ . In steady state the average energy of the *system* returns to its initial value after one cycle[74] so that  $\langle E_5 \rangle = \langle E_1 \rangle$ . From this it follows immediately that  $Q_c + Q_h + W = 0$ , i.e. the first law of thermodynamics is obeyed. There is no instantaneous energy conservation of *internal* energy, as energy may be temporarily stored in the interaction field or in the work repository.

In the two-stroke engine shown in Fig 1b the engine consists of two parts (e.g. two qubits) [54]. One part may couple only to the hot bath and the other may couple only to the cold bath. In the first stroke both parts interact with their bath (but do not necessarily reach equilibrium). In the second unitary stroke the two engine parts are disconnected from the baths and are coupled to each other. They undergo a mutual unitary evolution and work is extracted in the process.

In the continuous engine shown in Fig. 1c the two baths and the external interaction field are connected continuously. For example, in the three level laser system shown in Fig 1c the laser light represented by  $\mathcal{H}_w(t)$  generates stimulated emission that extracts work from the system. This system was first studied in thermodynamics context in [55], while a more comprehensive analysis of the system was given in [56]. It is imperative that the external field is time-dependent. If it is time-independent the problem becomes a pure heat transport problem where  $Q_h = -Q_c \neq 0$ . In heat transport the interaction field merely “dresses” the level so that the baths see a slightly modified system. The Lindblad generators are modified accordingly and heat flows without extracting or consuming work [57]. Variations on these

engine types may emerge due to realization constraints. For example, in the two stroke engine the baths may be continuously connected. This variation and others can still be analyzed using the tools presented in this paper.

### C. Efficiency vs. work and heat

Since the early days of Carnot, efficiency received considerable attention for two main reasons. First, this quantity is of great interest from both theoretical and practical points of view. The second reason is that efficiency satisfies a universal bound that is independent of the engine details. The Carnot efficiency bound is a manifestation of the second law of thermodynamics. Indeed, for Markovian bath dynamics it was shown that quantum heat engines cannot exceed the Carnot efficiency [5]. Recently, a more general approach based on a fluctuation theorem for QHE showed that the Carnot bound still holds for quantum engines [53]. Studies in which higher than Carnot efficiency are reported [40], are interesting but they use non-thermal baths and therefore not surprisingly deviate from results derived in the thermodynamic framework that deals with thermal baths. For example, an electric engine is not limited to Carnot efficiency since its power source is not thermal. Although, the present work has an impact on efficiency as well, we focus on work and heat separately in order to unravel quantum effects. As will be exemplified later, in some elementary cases these quantum effects do not influence the efficiency.

### D. Bath description and Liouville space

The dynamics of the working fluid (system) interacting with the heat baths is described by Lindblad-Gorini-Kossakowski-Sudarshan (LGKS) master equation for the density matrix [58–60]:

$$d_t \rho = L(\rho) = -i[H_s, \rho] + \sum_k A_k \rho A_k^\dagger - \frac{1}{2} A_k^\dagger A_k \rho - \frac{1}{2} \rho A_k^\dagger A_k, \quad (1)$$

where the  $A_k$  operators depend on the temperature, relaxation time of the bath, system bath coupling, and also on the system Hamiltonian  $H_s$  [58]. This form already encapsulates within the Markovian assumption of no memory. The justification for these equations arises from a “microscopic derivation” in the weak system bath coupling limit [61]. In this derivation a weak interaction field couples the system of interest to a large system (the bath) with temperature  $T$ . This interaction brings the system into a Gibbs state at temperature  $T$ . The Lindblad thermalization operators  $A_k$  used for the baths are described in the next section

Equation (1) is a linear equation so it can always be rearranged into a vector equation. Given an index mapping  $\rho_{N \times N} \rightarrow |\rho\rangle_{1 \times N^2}$  the Lindblad equation now reads:

$$id_t |\rho\rangle = (\mathcal{H}_s + \mathcal{L}) |\rho\rangle, \quad (2)$$

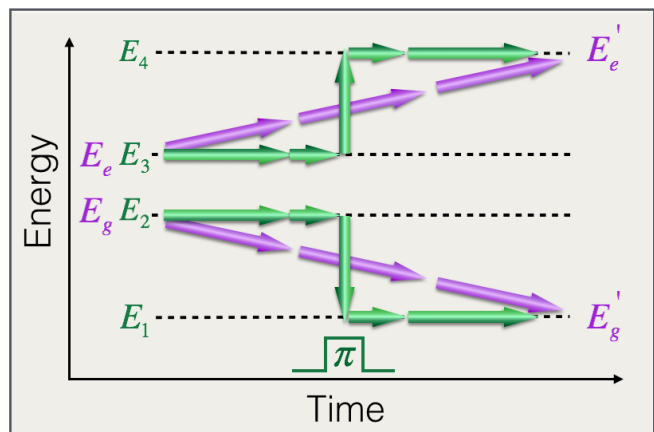


Figure 2: In the standard two-level Otto engine there are two-level  $E_{g,e}$  (purple) that change in time to  $E'_{g,e}$ . In the multilevel embedding framework, the levels ( $E_{1-4}$ ) are fixed in time (black dashed lines) but a time dependent field ( $\pi$  pulse, swap operation) transfer the population (green) to the other levels. For a swap operation the two schemes lead to the same final state and therefore are associate with the same work. Nonetheless, the multilevel scheme is more general since for weaker unitary transformation (instead of the  $\pi$  pulse), coherences are generated. We show that this type of coherences can significantly boost the power output of the engine.

where  $\mathcal{H}_s$  is an Hermitian  $N^2 \times N^2$  matrix that originates from  $H_s$ , and  $\mathcal{L}$  is a non Hermitian  $N^2 \times N^2$  matrix that originates from the Lindblad evolution generators  $A_k$ . This extended space is called Liouville space [62]. In this paper we will use calligraphic letters to describe operators in Liouville space and ordinary letters for operators in Hilbert space. For states, however,  $|A\rangle$  will denote a vector in Liouville space formed from  $A_{N \times N}$  by “vec-ing”  $A$  into a column in the same procedure  $\rho$  is converted into  $|\rho\rangle$ . A short review of Liouville space and some of its properties is given in appendix II.

While the Lindblad description works very well for sufficiently long times it fails for very short times where some of the approximation breaks down. In scales where the bath still has a memory of the system’s past states, the semi group property of the Lindblad equation no longer holds:  $|\rho(t+t')\rangle \neq e^{-i(\mathcal{H}_s + \mathcal{L})(t-t')} |\rho(t')\rangle$ . This will set a cutoff limit for the validity of the engine types equivalence in the Markovian approximation.

Next we introduce the multilevel embedding scheme that enables us to discuss various heat engines in the same physical setup.

### E. Multilevel embedding

Let the working substance of the quantum engine be an  $N$ -level system. These levels are fixed in time (i.e. they do not change as in Fig. 1a). For simplicity, the levels are non degenerate. We divide the energy levels into a cold manifold and a hot manifold. During the operation

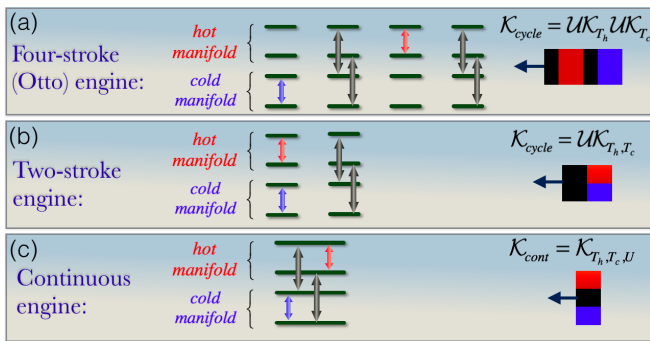


Figure 3: Representation of the three types of engines in the multilevel embedding framework. In this scheme the different engine types differ only in the order of coupling to the baths and work repository. Since the interactions and energy levels are the same for all engine types, a meaningful comparison of performance becomes possible.

of the engine the levels in the cold manifold interact only with the cold bath, and the hot manifold interact only with the hot bath. Each thermal coupling can be turned on and off as a function of time but the aliasing of a level to a manifold does not change in time.

If the manifolds do not overlap the hot and cold thermal operations commute and they can be applied at the same time or one after the other. The end result will be the same. Nevertheless, our scheme also includes the possibility that one level appears in both manifold. This is the case for the three-level continuous engine shown in Fig 1c. For simplicity, we exclude the possibility of more than one mutual level. If there are two or more overlapping levels there is an inevitable heat transport in steady state from the hot bath to the cold bath even in the absence of an external field that extract work. In the context of heat engines this can be interpreted as heat leak. This “no field - no transport” condition holds for many engines studied in the literature. Nonetheless, this condition is not a necessary condition for the validity of our results.

This manifold division seems sensible for the continuous engine and even for the two stroke engine in Fig 1b, but how can it be applied to the four stroke engine shown in Fig. 1a? The two levels interact with both baths and also change their energy value in time contrary to the assumption of fixed energy levels. Nevertheless, this engine is also incorporated in the multilevel embedding framework. Instead of two-levels as in Fig. 1a consider the four-level system shown in the dashed green lines in Fig 2.

Initially, only levels 2 and 3 are populated and coupled to the cold bath (2 & 3 are in the cold manifold). In the unitary stage an interaction Hamiltonian  $H_{swap}$  generates a full swap of populations and coherence according to the rule  $1 \leftrightarrow 2, 3 \leftrightarrow 4$ . Now levels 1 and 4 are populated and 2 and 3 are empty. Therefore, this system fully simulates the expanding level engine shown in Fig. 1a. At the same time this system satisfies the separation

into well defined time-independent manifolds as defined in the multilevel embedding scheme.

The full swap used to embed the traditional four-stroke Otto engine, is not mandatory and other unitary operations can be applied. This extension of the four-stroke scheme is critical for our work since the equivalence of engines appear when the unitary operation is fairly close to the identity transformation.

Figure 3 shows how the three engine types are represented in the multilevel embedding scheme. The advantage of the multilevel scheme now becomes clear. All three engine types can be described in the same physical system with the same baths and the same coupling to external fields (work extraction). The engine types differ only in the order of the coupling to the baths and to the work repository. While the thermal operations commute if the manifolds do not overlap, the unitary operation never commutes with the thermal strokes.

On the right of Fig. 3, we plotted a “brick” diagram for the evolution operator. Black stands for unitary transformation generated by some external field, while blue and red stand for hot and cold thermal coupling, respectively. When the bricks are on top of each other it means that they operate simultaneously. Now we are in position to derive the first main results of this paper: the thermodynamic equivalence of engine types in the quantum regime.

### III. CONTINUOUS AND STROKE ENGINE EQUIVALENCE

We first discuss the equivalence of continuous and four-stroke engines. Nevertheless, all the argument are valid for the two-stroke engines as well, as explained later on. Although our results are not limited to a specific engine model it will be useful to consider the simple engine shown in Fig. 4 . We will use this model to highlight a few points and also for numerical simulations. The Hamiltonian part of the system is:

$$H_0 + \cos(\omega t)H_w, \quad (3)$$

where  $H_0 = -\frac{\Delta E_h}{2} |1\rangle \langle 1| - \frac{\Delta E_c}{2} |2\rangle \langle 2| + \frac{\Delta E_c}{2} |3\rangle \langle 3| + \frac{\Delta E_h}{2} |4\rangle \langle 4|$ ,  $H_w = \epsilon(t) |1\rangle \langle 2| + \epsilon(t) |3\rangle \langle 4| + h.c.$  and  $\omega = \frac{\Delta E_h - \Delta E_c}{2}$ .

The driving frequency, that couples the system to the work repository is in resonance with the top and bottom energy gaps. The specific partitioning into hot and cold manifolds was chosen so that only one frequency (e.g. a single laser) is needed for implementing the system instead of two.

We assume that the Rabi frequency of the drive  $\epsilon$  is smaller than the decay time scale of the baths  $\epsilon \ll \gamma_c, \gamma_h$ . Under this assumption the dressing effect of the driving field on the system-bath interaction can be ignored. It is justified, then, to use “local” Lindblad operators obtained in the absence of a driving field [57, 63]. For plotting purposes (reasonable duty cycle) in the numerical

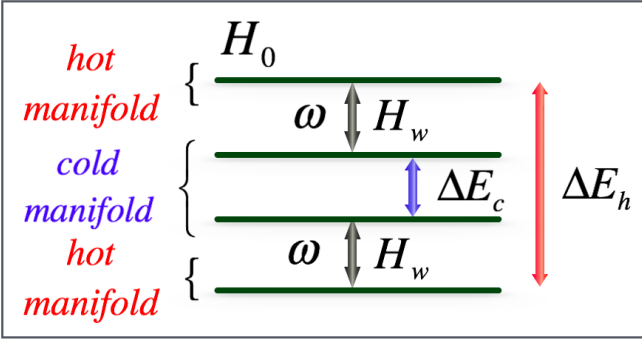


Figure 4: Illustration of the engine used in the numerical simulation. By changing the time order of the coupling to  $H_w$  and to thermal baths, all three type of engines can realized in the model.

examples we will often use  $\epsilon = \gamma_c = \gamma_h$ . While this poses no problem for stroke engines realizations, for experimental demonstration of equivalence with continuous engines one has to increase the duty cycle so that  $\epsilon \ll \gamma_c, \gamma_h$ . That is, the unitary stage should be made longer but with weaker driving field.

The Lindblad equation is given by (1) with the Hamiltonian (3) and with the following Lindblad operators:

$$\begin{aligned} A_1 &= \sqrt{\gamma_h} e^{-\frac{\Delta E_h}{2T_h}} |4\rangle \langle 1|, \\ A_2 &= \sqrt{\gamma_h} |1\rangle \langle 4|, \\ A_3 &= \sqrt{\gamma_c} e^{-\frac{\Delta E_c}{2T_c}} |3\rangle \langle 2|, \\ A_4 &= \sqrt{\gamma_c} |2\rangle \langle 3|. \end{aligned}$$

In all the numerical simulation we use  $\Delta E_h = 4$ ,  $\Delta E_c = 1$ ,  $T_h = 5$ ,  $T_c = 1$ . The interaction with the baths or with work repository can be turned on and off at will.

Starting with the continuous engine, we choose a unit cell that contains exactly  $6m$  ( $m$  is an integer) complete cycles of the drive ( $\tau_d = 2\pi/\omega$ ) so that  $\tau_{cyc} = 6m\tau_d$ . The difference between the engine cycle time and the cycles of the external drive, will become clear in stroke engines (also the factor of six will be clarified).

For the validity of the secular approximation used in the Lindblad microscopic derivation [58], the evolution time scale must satisfy  $\tau \gg \frac{2\pi}{\min(\Delta E_h, \Delta E_c)}$ . Therefore  $m$  must satisfy  $m \gg \frac{\omega}{\min(\Delta E_h, \Delta E_c)}$ . Note that if the Lindblad description is obtained from a different physical mechanism (e.g. thermalizing collisions) then this condition is not required.

Next we transform to the interaction picture (denoted by tilde) using the transformation  $\mathcal{U} = e^{-i\mathcal{H}_0 t}$ , and perform the rotating wave approximation (RWA) by dropping terms oscillating in frequency of  $2\omega$ . For the RWA to be valid the amplitude of the field must satisfy  $\epsilon \ll \omega$ . The resulting Liouville space super Hamiltonian is:

$$\tilde{\mathcal{H}} = \mathcal{L}_c + \mathcal{L}_h + \frac{1}{2}\mathcal{H}_w. \quad (4)$$

Note that  $\mathcal{L}_{h,c}$  were not modified by the transformation to the rotating system since  $[\mathcal{L}_{h,c}, \mathcal{H}_0] = 0$  in the microscopic derivation[75]. Now that we have established a regime of validity and the super Hamiltonian that governs the system, we can turn to the task of transforming from one engine type to other types and study what properties change in this transformation. The engine type transformation is based on the Strang decomposition [64] for two non commuting operators  $\mathcal{A}$  and  $\mathcal{B}$  (the operators may not be Hermitian):

$$e^{(\mathcal{A}+\mathcal{B})dt} = e^{\frac{1}{2}\mathcal{A}dt} e^{\mathcal{B}dt} e^{\frac{1}{2}\mathcal{A}dt} + O(s^3) \cong e^{\frac{1}{2}\mathcal{A}dt} e^{\mathcal{B}dt} e^{\frac{1}{2}\mathcal{A}dt}, \quad (5)$$

where  $s = (\|\mathcal{A}\| + \|\mathcal{B}\|)dt$  must be small for the expansion to be valid.  $\|\mathcal{A}\|$  is the spectral norm (or operator norm) of  $\mathcal{A}$ , and it is the largest singular value of  $\mathcal{A}$ ,  $\|\mathcal{A}\| = \max \sqrt{\text{eig}(\mathcal{A}\mathcal{A}^\dagger)}$ [65]. For Hermitian operators with eigenvalues  $\lambda_{\mathcal{A},i}$  the spectral norm is  $\max(|\lambda_{\mathcal{A},i}|)$ . In Appendix I we derive the condition  $s \ll \frac{1}{2}\hbar$  for the validity of (5). We will use the symbol  $\cong$  to denote equality with correction  $O(s^3)$ . Let the evolution operator of the continuous engine over the chosen cycle time  $\tau_{cyc} = 6m\tau_d$  be:

$$\tilde{\mathcal{K}}^{\text{cont}} = e^{-i\tilde{\mathcal{H}}\tau_{cyc}}. \quad (6)$$

By first splitting  $\mathcal{L}_c$  and then splitting  $\mathcal{L}_h$  we get:

$$\begin{aligned} \tilde{\mathcal{K}}^{\text{4 stroke}} &= e^{-i(3\mathcal{L}_c)\frac{\tau_{cyc}}{6}} e^{-i(\frac{3}{2}\mathcal{H}_w)\frac{\tau_{cyc}}{6}} e^{-i(3\mathcal{L}_h)\frac{\tau_{cyc}}{3}} \\ &\times e^{-i(\frac{3}{2}\mathcal{H}_w)\frac{\tau_{cyc}}{6}} e^{-i(3\mathcal{L}_c)\frac{\tau_{cyc}}{6}}. \end{aligned} \quad (7)$$

Note that the system is periodic so the first and last stages are two parts of the same thermal stroke. Consequently (7) describes an evolution operator of a four stroke engine, where the unit cell is symmetric. This splitting is illustrated in Fig. 5a and Fig. 5b. There are two thermal strokes and two work strokes that together constitute an evolution operator that describes a four-stroke engine. The cumulative evolution time as written above is  $(m + m + 2m + m + m)\tau_d = 6m\tau_d = \tau_{cyc}$ . Yet, to maintain the same cycle time as chosen for the continuous engine, the coupling to the baths and field were multiplied by three. In this four-stroke engine each thermal or work stroke operates in total only a third of the cycle time compared to the continuous engine. Hence, the coupling must be three times larger in order to generate the same evolution.

By virtue of the Strang decomposition  $\tilde{\mathcal{K}}^{\text{4 stroke}} \cong \tilde{\mathcal{K}}^{\text{cont}}$  if  $s \ll 1$ . The *action parameter*  $s$  of the engine is defined as  $s = \int_{-\tau_{cyc}/2}^{\tau_{cyc}/2} \|\tilde{\mathcal{H}}\| dt = (\frac{1}{2}\|\mathcal{H}_w\| + \|\mathcal{L}_h\| + \|\mathcal{L}_c\|)\tau_{cyc}$ . Although we used  $\hbar = 1$  units, note that  $s$  has dimensions of  $\hbar$  and therefore the relation  $\tilde{\mathcal{K}}^{\text{4 stroke}} \cong \tilde{\mathcal{K}}^{\text{cont}}$  holds only when the engine action is small compared to  $\hbar$ . This first appearance of a quantum scale will be discussed later on.

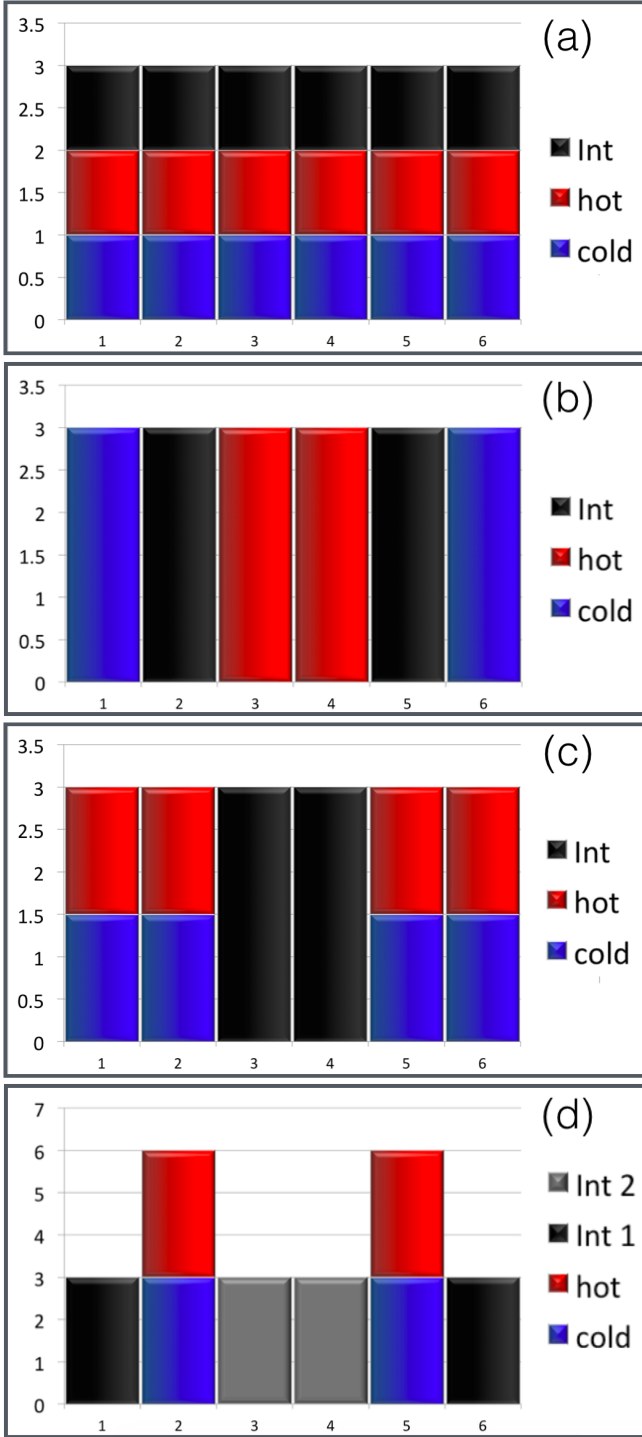


Figure 5: (color online) Illustration of the splitting of the evolution operator of the continuous engine (a), into a four-stroke engine (b), a two-stroke engine (c), and a two-field four-stroke engine (d). The horizontal axis corresponds to time as before. The size of the brick corresponds to the strength of coupling to the work repository or to the baths. The symmetric rearrangement theorem ensures that in the limit of small action, any rearrangement that is symmetric with respect to the center, and conserves the area of each color does not change the total power and heat.

### A. Dynamical aspect of the equivalence

Before discussing the thermodynamics properties of the engine we point out that  $\tilde{\mathcal{K}}^{4 \text{ stroke}} \cong \tilde{\mathcal{K}}^{\text{cont}}$  has two immediate important consequences. First both engines have the same steady state solution over one cycle  $|\tilde{\rho}_s\rangle$ :

$$\tilde{\mathcal{K}}^{4 \text{ stroke}}(\tau_{cyc})|\tilde{\rho}_s\rangle \cong \tilde{\mathcal{K}}^{\text{cont}}(\tau_{cyc})|\tilde{\rho}_s\rangle = |\tilde{\rho}_s\rangle, \quad (8)$$

$$(\mathcal{L}_c + \mathcal{L}_h + \frac{1}{2}\mathcal{H}_w)|\tilde{\rho}_s\rangle = 0. \quad (9)$$

At time instances that are not an integer multiples  $\tau_{cyc}$ , the states of the engines will differ significantly ( $O(s^1)$ ) since  $\tilde{\mathcal{K}}^{4 \text{ stroke}}(t < \tau_{cyc}) \neq \tilde{\mathcal{K}}^{\text{cont}}(t < \tau_{cyc})$ . That is, the engines are still significantly different from each other. The second consequence is that the two engines have the same transient modes as well. When monitored at multiple of  $\tau_{cyc}$  both engines will have the same relaxation dynamics to steady state if they started from the same initial condition. In the reminder of the paper, when the evolution operator is written without a time tag, it means we consider the evolution operator of a complete cycle.

### B. Thermodynamic aspect of the equivalence

The equivalence of the one cycle evolution operators of the two engines does not immediately imply that the engines are thermodynamically equivalent. Generally, in stroke engines the heat and work depend on the dynamics of the state inside the cycle which is very different ( $O(s^1)$ ) from the constant state of the continuous engine. However, in this section we show that all thermodynamics properties are equivalent in both engines up to  $O(s^3)$  corrections, similarly to the evolution operator. We start by evaluating the work and heat in the continuous engine. By considering infinitesimal time elements where  $\mathcal{L}_c, \mathcal{L}_h$  and  $\mathcal{H}_w$  operate separately, one obtains that the heat and work currents are [76]  $j_{c(h)} = \langle H_0 | \mathcal{L}_{c(h)} | \tilde{\rho}_s(t) \rangle$  and  $j_w = \langle H_0 | \frac{1}{2}\mathcal{H}_w | \tilde{\rho}_s(t) \rangle$ . In the continuous engine the steady state satisfies  $|\tilde{\rho}_s(t)\rangle = |\tilde{\rho}_s\rangle$  so the total heat and work in steady state in one cycle are:

$$W^{\text{cont}} = \left\langle H_0 \left| \frac{1}{2}\mathcal{H}_w \right| \tilde{\rho}_s \right\rangle \tau_{cyc}, \quad (10)$$

$$Q_{c(h)}^{\text{cont}} = \langle H_0 | \mathcal{L}_{c(h)} | \tilde{\rho}_s \rangle \tau_{cyc}. \quad (11)$$

These quantities should be compared to the work and heat in the four-stroke engine. Instead of carrying out the explicit calculation for this specific four-stroke splitting we use the symmetric rearrangement theorem (SRT) derived in Appendix III. Symmetric rearrangement of a Hamiltonian means is a change in the order of couplings  $\epsilon(t), \gamma_c(t), \gamma_h(t)$  that satisfies  $\int \epsilon(t)dt = \text{const}$ ,  $\int \gamma_c(t)dt = \text{const}$ ,  $\int \gamma_h(t)dt = \text{const}$  and  $\epsilon(t) = \epsilon(-t), \gamma_c(t) = \gamma_c(-t), \gamma_h(t) = \gamma_h(-t)$ .  $\mathcal{H}^{II \text{ stroke}}(t)$ ,  $\mathcal{H}^{IV \text{ stroke}}(t)$  and any other super Hamiltonian obtained using the Strang splitting of the continuous engine, are

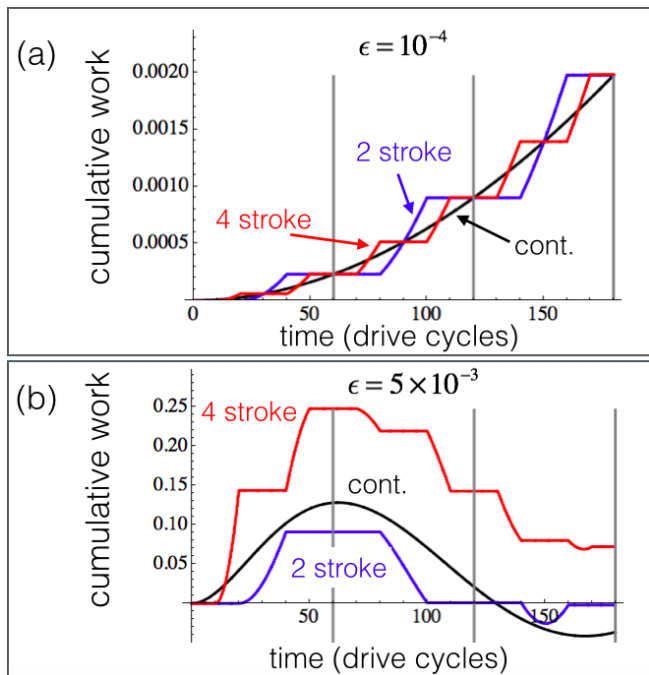


Figure 6: The equivalence of heat engine types in transient evolution when the engine action is small compared to  $\hbar$ . (a) The cumulative power transferred to the work repository is plotted as a function of time. All engines start in the excited state  $|4\rangle$ , which is very far from the steady state of the system. At complete engine cycles (vertical lines) the power in all engines is the same. (b) Once the action is increased (here the field  $\epsilon$  was increased), the equivalence no longer holds.

examples of symmetric rearrangements. The SRT exploits the symmetry of the Hamiltonian to show that symmetric rearrangement change heat and work only in  $O(s^3)$ . In the Appendix III we show that

$$W^4 \text{ stroke} \cong W^{\text{cont}}, \quad (12)$$

$$Q_{c(h)}^4 \text{ stroke} \cong Q_{c(h)}^{\text{cont}}. \quad (13)$$

Thus, we conclude that up to  $s^3$  corrections, the engines are thermodynamically equivalent. When  $s \ll 1$ , work, power heat and efficiency converge to the same value for all engine types. Clearly, inside the cycle the work and heat in the two engine are significantly different ( $O(s^1)$ ) but after a complete cycle they become equivalent. The symmetry makes this equivalent more accurate as it holds up to  $s^3$  (rather  $s^2$ ). Interestingly the work done in the first half of the cycle is  $\frac{1}{2}W^{\text{cont}} + O(s^2)$ . However, when the contribution of the other half is added the  $s^2$  correction cancels out and (12) is obtained (see Appendix III).

We emphasize that the SRT and its implications (12),(13) are valid for transients and for any initial state - not just for steady state operation. In Fig. 6a we show the cumulative work as a function of time for a four-stroke engine and a continuous engine. The vertical lines indicate complete cycle of the four-stroke engine.

In addition to the parameter common to all examples specified before, we used  $\epsilon = \gamma_c = \gamma_h = 10^{-4}$  and the equivalence of work at the vertical lines is apparent. In Fig. 6b the field and thermal coupling was increased to  $\epsilon = \gamma_c = \gamma_h = 5 \times 10^{-3}$ . Now the engines perform differently even at the end of each cycle. This example is a somewhat extreme situation where the system changes quite rapidly (consequence of the initial state we chose). In other cases, such as steady state operation, the equivalence can be observed for much larger action values.

The splitting used in (7) was based on first splitting  $\mathcal{L}_c$  and then  $\mathcal{H}_w$ . Other engines can be obtained by different splitting of  $\tilde{\mathcal{K}}^{\text{cont}}$ . For example, consider the two-stroke engine obtained by splitting  $\mathcal{L}_c + \mathcal{L}_h$ :

$$\tilde{\mathcal{K}}^2 \text{ stroke} = e^{-i\frac{3}{2}(\mathcal{L}_c + \mathcal{L}_h)\frac{\tau_{\text{cyc}}}{3}} e^{-i(\frac{3}{2}\mathcal{H}_w)\frac{\tau_{\text{cyc}}}{3}} e^{-i\frac{3}{2}(\mathcal{L}_c + \mathcal{L}_h)\frac{\tau_{\text{cyc}}}{3}}. \quad (14)$$

Note that in the two-stroke engine the thermal coupling has to be  $\frac{3}{2}$  stronger compared to the continuous case in order to provide the same action. Using the SRT we obtain the complete equivalence relations of the three main engine types[77]:

$$W^2 \text{ stroke} \cong W^4 \text{ stroke} \cong W^{\text{cont}}, \quad (15)$$

$$Q_{c(h)}^2 \text{ stroke} \cong Q_{c(h)}^4 \text{ stroke} \cong Q_{c(h)}^{\text{cont}}, \quad (16)$$

$$\tilde{\mathcal{K}}^2 \text{ stroke} \cong \tilde{\mathcal{K}}^4 \text{ stroke} \cong \tilde{\mathcal{K}}^{\text{cont}}. \quad (17)$$

Another type of engine exists when the interaction with the work repository is carried out by two physically distinct couplings. This happens naturally if  $E_4 - E_3 \neq E_2 - E_1$  so that two different driving lasers have to be used and the Hamiltonian is  $H_0 + \cos((E_2 - E_1)t)H_{w1} + \cos((E_4 - E_3)t)H_{w2}$ . In such cases, one can make the splitting shown in Fig. 5d. In this numerical example we use:  $H_{w1} = \epsilon(t)|1\rangle\langle 2| + h.c.$  and  $H_{w2} = \epsilon(t)|3\rangle\langle 4| + h.c.$  Since there are two different work strokes in addition to the thermal stroke this engine constitute a four-stroke engine which differce.

### C. Power and energy flow balance

The average power and heat flow in the equivalence regime are independent of the cycle time:

$$P_W = \frac{W}{\tau_{\text{cyc}}} = \left\langle H_0 \left| \frac{1}{2}\mathcal{H}_w \right| \tilde{\rho}_s \right\rangle, \quad (18)$$

$$J_{c(h)} = \frac{Q_{c(h)}}{\tau_{\text{cyc}}} = \langle H_0 | \mathcal{L}_{c(h)} | \tilde{\rho}_s \rangle. \quad (19)$$

Using the steady state definition (9) one obtains the steady state energy balance equation:

$$P_w + J_c + J_h = 0. \quad (20)$$

Equation (20) does not necessarily hold if the system is not in steady state as energy may be temporarily stored in the baths or in the work repository.



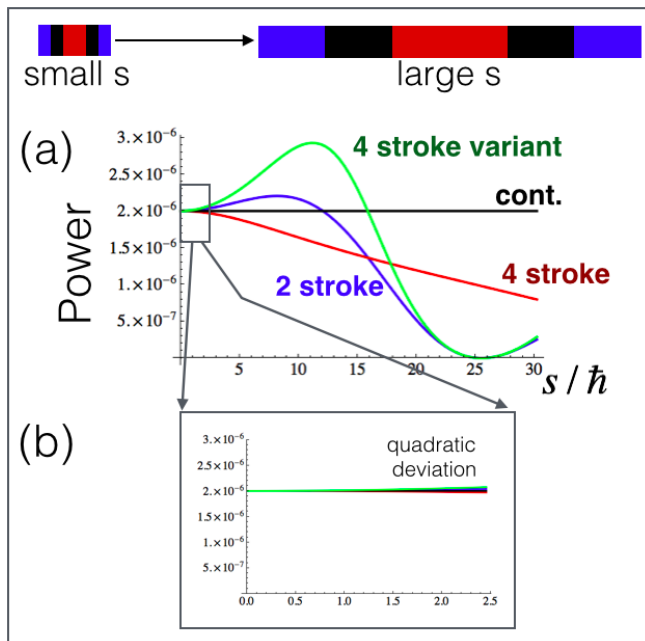


Figure 7: Power as a function of action for various engine types in steady state. The 4 stroke variant (green) is described at the end of Sec. III B. The action is increased by increasing the strokes duration (top illustration). (a) For large action with respect to  $\hbar$ , the engines significantly differ in performance. In this example all engines have the same efficiency, but they extract different amounts of heat from the hot bath. (b) In the equivalence regime where the action is small, all engine types exhibit the same power and also the same heat flows. The condition  $s < \hbar/2$  that follows from the Strang decomposition agrees with the observed regime of equivalence. The time symmetric structure of the engines causes the deviation from equivalence to be quadratic in the action.

Figure 7 shows the power in steady state as a function of the action. The action is increased by increasing the time duration of each stroke (see top illustration in Fig. 7). The field and the thermal coupling are  $\epsilon = \gamma_h = \gamma_c = 5 \times 10^{-4}$ . The coupling strengths to the bath and work repository are not changed. When the engine action is large compared to  $\hbar$ , the engines behave very differently (Fig. 7a). On the other hand, in the equivalence regime, where  $s$  is small with respect to  $\hbar$ , the power of all engine types converges to the same value. In the equivalence regime the power rises quadratically with the action since the correction to the power is  $s^3/\tau_{cyc} \propto \tau_{cyc}^2$ . This power plateau in the equivalence regime is a manifestation of quantum interference effects (coherence in the density matrix), as will be further discussed in the next section.

The behavior of different engines for large action with respect to  $\hbar$  is very rich and strongly depends on the ratio between the field and the baths coupling strength. For example, if the field is amplified then for some parameter the four-stroke engine can produce more power than the continuous and two stroke engine. Some features of this diverse dynamics will be discussed elsewhere.

Finally we comment that the same formalism and results can be extended for the case the drive that is slightly detuned from the gap.

#### D. Lasing condition via the equivalence to two-stroke engine

Laser medium can be thought of as continuous engine where the power output is light amplification. It is well known that lasing requires population inversion. Scovil et. al [55] were the first to show the relation between population inversion lasing condition, and the Carnot efficiency.

Using the equivalence principle, presented here, the most general form of the lasing condition can be obtained without any reference to light-matter interaction.

Let us start by decomposing the continuous engine into an equivalent two-stroke engine. For simplicity, it is assumed that the hot and cold manifolds have some overlap so that in the absence of the driving field this bath leads the system to a unique steady state  $\rho_0$ . If the driving field is tiny with respect to the thermalization rates then the system will be very close to  $\rho_0$  in steady state.

To see when  $\rho_0$  can be used for work extraction we need to discuss passive states. A passive state is a state that is diagonal in the energy basis, and with populations that decreases monotonically with the energy [66]. The energy of a passive state cannot be decreased (or work cannot be extracted from the system) by applying some unitary transformation (the Hamiltonian after the transformation is the same as it was before the transformation) [42, 66]. Thus, if  $\rho_0$  is passive, work cannot be extracted from the device regardless of the details of the driving field (as long as it is weak and the equivalence holds).

A combination of thermal baths will lead to an energy diagonal  $\rho_0$ . Consequently, to enable work extraction, passivity must be broken by population inversion. Therefore, we obtain the standard population inversion condition. Note that the derivation does not require Einstein rate equation and any information on the processes of emission and absorption of photons.

Furthermore, it now becomes clear that if “coherent baths” are used [40] so that  $\rho_0$  is no longer diagonal in the energy basis (and therefore no longer passive) it is possible to extract work even without population inversion.

In conclusion, using the equivalence principle it is possible to import known results from work extraction in stroke schemes to continuous machines.

## IV. QUANTUM THERMODYNAMIC SIGNATURE

Can thermodynamic measurement reveal quantum effects in the engine? To answer this we first need to define

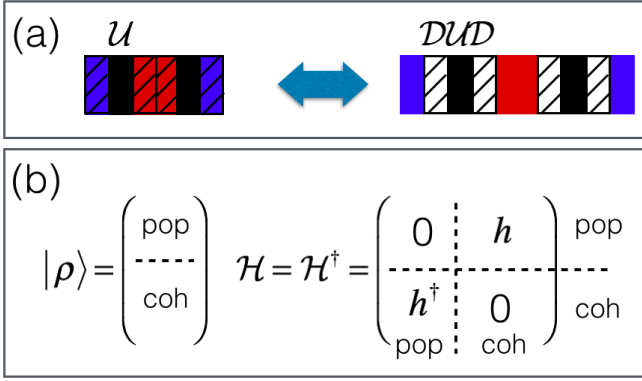


Figure 8: (a left) Dephasing operations (slanted line, operator  $\mathcal{D}$ ) commute with thermal baths so the dephased engine in (a) left, is equivalent to the one on the right. In the new engine the unitary evolution is replaced by  $\mathcal{DUD}$ . If  $\mathcal{D}$  eliminates all coherences, the effect of  $\mathcal{DUD}$  on the populations can always be written as a doubly stochastic operator. (b) Any Hermitian Hamiltonian in Liouville space has the structure shown in (b). Thus, first order changes in populations critically depend on the existence of coherence.

the corresponding classical engine.

The term “classical” engine is rather ambiguous. There are different protocols of modifying the system so that it behaves classically. To make a fair comparison to the fully quantum engine we look for the minimal modification that satisfies the following conditions:

1. The dynamics of the device should be fully described using population dynamics (no coherences, no entanglement).
2. The modification should not alter the energy levels of the system, the couplings to the baths, and the coupling to the work repository.
3. The modification should not introduce a new source of heat or work.

To satisfy the first requirement we introduce a dephasing operator that eliminates the coherences [78] and leads to a stochastic description of the engine. Clearly, dephasing operators satisfy the second requirement. To satisfy the third requirement we require “pure dephasing”; a dephasing in the energy basis. The populations in the energy basis are invariant to this dephasing operation. Such a natural source of energy basis dephasing emerges if there is some scheduling noise [67]. That is, if there is some error in the switching time of the strokes.

Let us define a “quantum-thermodynamic signature” as a signal that is impossible to produce by the corresponding classical engine as defined above.

Our goal is to derive a threshold for power output that a stochastic engine cannot exceed but a coherent quantum engine can.

Before analyzing the effect of decoherence it is instructive to distinguish between two different work extraction mechanisms in stroke engines.

### A. Coherent and stochastic work extraction mechanisms

Let us consider the work done in the work stroke of a two-stroke engine (as in Fig. 5c):

$$W = \langle H_0 | e^{-i\frac{1}{2}\mathcal{H}_w\tau_w} | \tilde{\rho} \rangle.$$

Writing the state as a sum of population and coherences  $|\tilde{\rho}\rangle = |\tilde{\rho}_{pop}\rangle + |\tilde{\rho}_{coh}\rangle$  we get:

$$W = \left\langle H_0 \left| \sum_{n=1} \frac{(-i\frac{1}{2}\mathcal{H}_w\tau_w)^{2n-1}}{(2n-1)!} \right| \tilde{\rho}_{coh} \right\rangle + \left\langle H_0 \left| \sum_{n=1} \frac{(-i\frac{1}{2}\mathcal{H}_w\tau_w)^{2n}}{(2n)!} \right| \tilde{\rho}_{pop} \right\rangle. \quad (21)$$

This result follows from the generic structure of Hamiltonians in Liouville space. Any  $\mathcal{H}$  that originates from an Hermitian Hamiltonian in Hilbert space (in contrast to Lindblad operators as a source) has the structure shown in Fig 8b (see Appendix II for Liouville space derivation of this property). That is, it connects only populations to coherences and vice versa, but it cannot connect populations to populations directly [79]. In addition, since  $\langle H_0 |$  acts as a projection on population space one gets that odd powers of  $\mathcal{H}_w$  can only operate on coherences and even powers can only operate on populations. Thus, the power can be extracted using two different mechanisms. A coherent mechanism that operates on coherences and a stochastic mechanism that operates on populations.

The effect of the “stochastic” terms  $\sum_{n=1} \frac{(-i\frac{1}{2}\mathcal{H}_w\tau_w)^{2n}}{(2n)!}$  on the populations are equivalently described by a single doubly stochastic operator. If there are no coherences (next section) this leads to a simple interpretation in terms of full swap events that take place with some probability.

Continuous engines, on the other hand, have only coherent work extraction mechanism. This can be seen from the expression for their work output

$$P^{\text{cont}} = \left\langle H_0 \left| \frac{1}{2}\mathcal{H}_w \right| \tilde{\rho} \right\rangle = \left\langle H_0 \left| \frac{1}{2}\mathcal{H}_w \right| \tilde{\rho}_{coh} \right\rangle, \quad (22)$$

where again we used the population projection property of  $\langle H_0 |$ , and the structure of  $\mathcal{H}_w$  (Fig. 8b). We conclude that in contrast to stroke engines, continuous engines have no stochastic work extraction mechanism. This difference stems from the fact that in steady state the state is stationary in continuous engines. Consequently, there are no higher order terms that can give rise to a population-population stochastic work extraction mechanism. This is a fundamental difference between stroke engines and continuous engines. This effect is pronounced outside the equivalence regime where the stochastic terms become important (see Sec. V).

## B. Engines subjected to pure dephasing

Consider the engine shown in Fig 8a. The slanted lines on the baths indicate that there is an additional dephasing mechanism that takes place in parallel to the thermalization[80]. Let us denote the evolution operator of the pure dephasing by  $\mathcal{D}$ . In principle, to analyze the deviation from the coherent quantum engine, first the steady state has to be solved and then work and heat can be compared. Even for simple systems this is difficult task. Hence, we shall take a different approach and derive a power upper bound for stochastic engines. It is important that the bound will contain only quantities that are unaffected by the level of coherence in the system. For example, average energy or dipole expectation values, do contain information on the coherence. We construct a bound in terms of the parameters of the system (e.g. the energy levels, coupling strengths, etc.), an is independent of the state of the system. In the pure dephasing stage the energy does not change. Hence, the total energy change in the  $\mathcal{DUD}$  stage is associated with work.

Let  $\mathcal{D}_{comp} = |pop\rangle\langle pop|$  be a projection operator on the population space. This operator generates a complete dephasing that eliminates all coherences. In such case, the leading order in the work expression becomes

$$\begin{aligned} W &= \left\langle H_0 \left| \mathcal{D}_{comp} e^{-i\frac{1}{2}\mathcal{H}_w\tau_w} \mathcal{D}_{comp} \right| \tilde{\rho} \right\rangle \\ &= \frac{\tau_w^2}{8} \langle H_0 | \mathcal{H}_w^2 | \tilde{\rho}_{pop} \rangle + O(s^4), \end{aligned} \quad (23)$$

where we used  $\langle H_0 | \mathcal{D} = \langle H_0 |$  and  $\mathcal{D}_{comp} |\tilde{\rho}\rangle = |\tilde{\rho}_{pop}\rangle$ . Since  $\mathcal{D}_{comp}$  eliminates coherences,  $W$  does not contain a linear term in time. Next by using the following relation:  $\langle H_0 | B | \rho \rangle \leq \sqrt{\langle H_0 | H_0 \rangle \langle \rho | \rho \rangle} \|B\|$ ,  $\sqrt{\langle H_0 | H_0 \rangle} = \sqrt{\text{tr}(H_0^2)}$ , we find that for  $s \ll \hbar$  the power of a stochastic engine satisfies:

$$\begin{aligned} P_{stoch} &\leq \frac{z}{8} \sqrt{\text{tr}(H_0^2) - \text{tr}(H_0)^2} \Delta_w^2 d^2 \tau_{cyc}, \quad (24) \\ z = 1 &\quad \text{two-stroke} \\ z = 1/2 &\quad \text{four-stroke} \end{aligned}$$

where  $\Delta_w$  is the gap of the interaction Hamiltonian (maximal eigenvalue minus minimal eigenvalue of  $H_w$ ), and  $d$  is the duty cycle - the fraction of time dedicated to work extraction (e.g.  $d = 1/3$  in all the examples in this paper). We also used the fact that  $\langle \rho_{pop} | \rho_{pop} \rangle$  is always smaller than the purity  $\langle \rho | \rho \rangle$  and therefore smaller than one. Note that, as we required, this bound is state-independent, and the right hand side of (24) contains no information on the coherences in the system. As shown earlier, in coherent quantum engines (in the equivalence regime) the work scales linearly with  $\tau_{cyc}$  (see (10) and (12)) and therefore the power is constant as a function of  $\tau_{cyc}$ . When there are no coherences the power scales linearly with  $\tau_{cyc}$ .

Numerical results of power as function of cycle time are shown in Fig. 9. The power is not plotted as function of action as before, because at the same cycle time the coherent engine and dephased engine have different action. The action of the dephased engine is

$$s_{deph} = (\|\mathcal{L}_c\| + \|\mathcal{L}_h\| + \left\| \frac{1}{2}\mathcal{H}_w \right\| + \|\mathcal{L}_{dephasing}\|) \tau_{cyc}. \quad (25)$$

If the dephasing is significant the action is large and equivalence cannot be observed. That is, a fully stochastic engine in quantum system have large action and cannot satisfy  $s \ll \hbar$ .

The chosen coherence time is  $100\tau_d$ . When the cycle time is small with respect to the coherence time, equivalence is observed. Yet, the power is significantly smaller compared to the fully coherent case. For longer cycles the decoherence starts to take effect, and the expected linear power growth is observed. The stochastic power bounds for a two-stroke engine (dashed-blue), and for a four-stroke engine (dashed-red) define a power regime (shaded area) that is inaccessible to fully stochastic engines. Thus, any power measurement in this regime unequivocally indicates the presence of quantum coherences in the engine. Note, that to measure power the work repository is measured and not the engine. Furthermore, the engine must operate for many cycles to reduce fluctuations in the accumulated work. To calculate the average power the accumulated work is divided by the total operation time and compared to the stochastic power threshold (24).

Note that had we chosen complete dephasing then the power output of the continuous engine would have been zero as expected from (22).

In summary, quantum thermodynamics signature in stroke engines can be observed in the weak action limit.

## V. THE OVER THERMALIZATION EFFECT IN COHERENT QUANTUM HEAT ENGINE

In all the numerical examples studied so far, the unitary action and the thermal action were roughly comparable for reason that will soon become clear. In this section we study some generic features that take place when the thermal action takes over.

Let us now consider the case where the unitary contribution to the action  $\|\mathcal{H}_w\| \tau$  is small with respect to  $\hbar$ . All the time intervals are fixed but we can control the thermalization rate  $\gamma$  (for simplicity, we assume it is the same value for both baths). Common sense suggests that increasing  $\gamma$  should increase the power output. At some stage this increase will stop since the system will already reach thermal equilibrium with the bath (or baths in two-stroke engines). Yet, Fig. 10 shows that there is a very distinctive peak where an optimal coupling takes place. That is, in some cases less thermalization leads to more power. We call this effect over thermalization. This effect is generic and not unique to the specific model

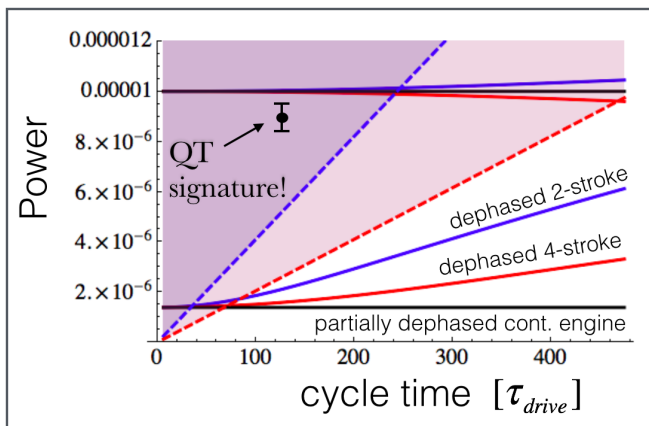


Figure 9: The output of the three types of engines (two-stroke blue, four stroke red, continuous black) with and without dephasing (same as Fig. 7b). The dephasing time is  $100\tau_{drive}$ . Well above the dephasing time ( $\sim 200\tau_{drive}$ ) the power grows linearly as expected from stochastic engines (three bottom solid lines). Below the dephasing time ( $\sim 20\tau_{drive}$ ) equivalence is observed. Yet the power is significantly lower compared to the coherent engine (top three solid lines). The dashed lines show the stochastic upper bound on the power for two-stroke (dashed-blue) and four-stroke (dashed-red) engines. Any power measurement in the shaded area of each engine indicates the presence of quantum interference in the engine. This plot also demonstrates that for weak couplings (low action) coherent engines produce much more power compared to stochastic dephased engines.

used in the numerical simulations. The parameter used for the plot are  $\epsilon = \gamma_c = \gamma_h = 2 \times 10^{-4}$  and the number of drive cycle per engine cycle is  $m = 600$ .

The peak is a consequence of the interplay between the two different work extraction mechanisms (see Sec. 4.1). For low  $\gamma$  the coherences in the system are significant and the leading term in the power is  $\langle H_0 | -i\frac{1}{2}\mathcal{H}_w | \tilde{\rho}_{coh} \rangle d$  (where  $d$  is the duty cycle). In principle, all Lindblad thermalization processes are associated with some level of decoherence. This decoherence generates an exponential decay of  $|\tilde{\rho}_{coh}\rangle$  that explains the decay on the right hand side of the peak. At a certain stage the linear term becomes so small that the stochastic second order term  $-\frac{1}{8}\langle H_0 | \mathcal{H}_w^2 | \tilde{\rho}_{pop} \rangle d^2\tau_{cyc}$  dominates the power.  $|\tilde{\rho}_{pop}\rangle$  eventually saturates for large  $\gamma$  and therefore the stochastic second order term leads to a power saturation. Interestingly, in the example shown in Fig. (V) we observe that the peak is obtained when  $\gamma$  and  $\epsilon$  are roughly equal. Of course, what really matters is the thermal action with respect to unitary action and not just the values of the parameter  $\gamma$  and  $\epsilon$ .

If thermalization occurs faster, the thermal stroke can be shortened and this increases the power. However, this effect is small with respect to the exponential decay of the coherences. We conclude that even without additional dephasing as in the previous section, excessive thermal coupling turns the engine into a stochastic machine. For small unitary action this effect severely de-

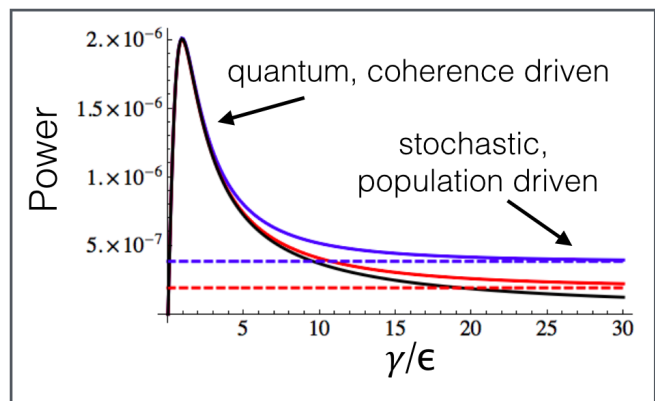


Figure 10: The over thermalization effect is the decrease of power when the thermalization rate is increased. Over thermalization degrades the coherent work extraction mechanism without effecting the stochastic work extraction mechanism. When the coherent mechanism gets weak enough, the power is dominated by the stochastic power extraction mechanisms and power saturation is observed (dashed lines). The continuous engine has no stochastic work extraction mechanism and therefore it decays to zero without reaching saturation.

grades the power output. The arguments presented here are valid for any small action coherent quantum engine.

## VI. CONCLUDING REMARKS

We identified coherent and stochastic work extraction mechanisms in quantum heat engines. While stroke engines have both, continuous engines only have the coherent mechanism. We introduced the “norm action” of the engine using Liouville space and showed that when this action is small compared to  $\hbar$  all three engine types are equivalent. This equivalence emerges because for small action only the coherent mechanism is important. Despite the equivalence, before the engine cycle is completed the state of the different engine type differ by  $O(s^1)$ . This holds true also for work and heat. Remarkably, at the end of each engine cycle a much more accurate  $O(s^3)$  equivalence emerges. Furthermore, the equivalence holds also for transient dynamics, even when the initial state is very far from the steady state of the engine. It was shown that for small action the coherent work extraction is considerably stronger than the stochastic work extraction mechanism. This enabled us to derive a power bound for stochastic engines that constitutes a quantum thermodynamics signature. Any power measurement that exceeds this bound indicated the presence of quantum coherence and the operation of the coherent work extraction mechanism.

The present derivation makes no assumption on the direction of heat flows and the sign of work. Thus our result are equally applicable to refrigerators and heaters.

It is interesting to try and apply these concepts of equivalence and quantum thermodynamic signatures to

more general scenarios: non Markovian baths, engines with non symmetric unit cell, and engines with correlation between different particles (entanglement and quantum discord). We conjecture that in multiple particle engines entanglement will play a similar role to that of coherence in single particle engines.

Work support by the Israeli science foundation. Part of this work was supported by the COST Action MP1209 'Thermodynamics in the quantum regime'.

### Appendix I - Strang decomposition validity

Let  $\mathcal{K}$  be an operator generated by two non commuting operators  $\mathcal{A}$  and  $\mathcal{B}$ :

$$\mathcal{K} = e^{(\mathcal{A}+\mathcal{B})dt}.$$

The splitted operator is

$$\mathcal{K}_s = e^{\frac{1}{2}\mathcal{A}dt} e^{\mathcal{B}dt} e^{\frac{1}{2}\mathcal{A}dt}.$$

Our goal is to quantify the difference between  $\mathcal{K}$  and  $\mathcal{K}_s$ ,  $\|\mathcal{K}_s - \mathcal{K}\|$  where  $\|\cdot\|$  stands for the spectral norm. In principle, other sub-multiplicative matrix norm can be used (such as the Hilbert Schmidt norm). However, the spectral norm captures more accurately aspects of quantum dynamics [68–71].  $\mathcal{K}$  can be expanded as:

$$\mathcal{K} = \sum \frac{(\mathcal{A} + \mathcal{B})^n dt^n}{n!}. \quad (26)$$

$\mathcal{K}_s$  on the other hand is:

$$\begin{aligned} \mathcal{K}_s &= \sum_{k,l,m=0}^{\infty} \frac{(\mathcal{A}/2)^k dt^k}{k!} \frac{\mathcal{B}^l dt^l}{l!} \frac{(\mathcal{A}/2)^m dt^m}{m!} \\ &= \sum_{n=0}^{\infty} \sum_{l=0}^n \sum_{k=0}^{n-l} \frac{(\mathcal{A}/2)^k}{k!} \frac{\mathcal{B}^l}{l!} \frac{(\mathcal{A}/2)^{n-l-k}}{(n-l-k)!} dt^n. \end{aligned} \quad (27)$$

Due to the symmetric splitting the terms up to  $n = 2$  (including  $n=2$ ) are identical for both operators. Therefore the difference can be written as

$$\begin{aligned} \|\mathcal{K}_s - \mathcal{K}\| &= \left\| \sum_{n=3}^{\infty} \sum_{l=0}^n \sum_{k=0}^{n-l} \frac{(\mathcal{A}/2)^k}{k!} \frac{\mathcal{B}^l}{l!} \frac{(\mathcal{A}/2)^{n-l-k}}{(n-l-k)!} dt^n \right. \\ &\quad \left. - \sum_{n=3}^{\infty} \frac{(\mathcal{A} + \mathcal{B})^n dt^n}{n!} \right\|. \end{aligned} \quad (28)$$

next we apply the triangle inequality and the sub-multiplicativity property and get:

$$\begin{aligned} \|\mathcal{K}_s - \mathcal{K}\| &\leq \left\| \sum_{n=3}^{\infty} \sum_{l=0}^n \sum_{k=0}^{n-l} \frac{\|\mathcal{A}/2\|^k}{k!} \frac{\|\mathcal{B}\|^l}{l!} \frac{\|\mathcal{A}/2\|^{n-l-k}}{(n-l-k)!} dt^n \right. \\ &\quad \left. + \sum_{n=3}^{\infty} \frac{(\|\mathcal{A}\| + \|\mathcal{B}\|)^n dt^n}{n!} \right\|. \end{aligned} \quad (29)$$

Using the binomial formula two times one finds

$$\begin{aligned} \sum_{n=3}^{\infty} \sum_{l=0}^n \sum_{k=0}^{n-l} \frac{\|\mathcal{A}/2\|^k}{k!} \frac{\|\mathcal{B}\|^l}{l!} \frac{\|\mathcal{A}/2\|^{n-l-k}}{(n-l-k)!} dt^n &= \\ \sum_{n=3}^{\infty} \frac{(\|\mathcal{A}\| + \|\mathcal{B}\|)^n dt^n}{n!}, \end{aligned} \quad (30)$$

and therefore

$$\begin{aligned} \|\mathcal{K}_s - \mathcal{K}\| &\leq 2 \sum_{n=3}^{\infty} \frac{(\|\mathcal{A}\| + \|\mathcal{B}\|)^n dt^n}{n!} \\ &= 2R_2[(\|\mathcal{A}\| + \|\mathcal{B}\|)dt]. \end{aligned} \quad (31)$$

The right hand side is the Taylor reminder of a power series of an exponential with as argument  $s = (\|\mathcal{A}\| + \|\mathcal{B}\|)dt$ . The Taylor reminder formula for the exponent function is  $R_k(x) = e^{\xi} \frac{|s|^{k+1}}{(k+1)!}$  where  $0 \leq \xi \leq 1$  (for now we assume  $s < 1$ ). Setting  $k = 2$  and  $\xi = 1$  (worst case), we finally obtain

$$\|\mathcal{K}_s - \mathcal{K}\| \leq \frac{e}{3} [(\|\mathcal{A}\| + \|\mathcal{B}\|)dt]^3 \leq s^3, \quad (32)$$

$$s = (\|\mathcal{A}\| + \|\mathcal{B}\|)dt. \quad (33)$$

To get an estimation where the leading non neglected term of  $\mathcal{K}$ ,  $(\mathcal{A} + \mathcal{B})^2 dt^2 / 2$  is larger then the reminder we require that

$$(\|\mathcal{A} + \mathcal{B}\|)^2 dt^2 / 2 \geq s^3. \quad (34)$$

Using the triangle inequality we get the estimated condition for the Strang decomposition:

$$s \leq 1/2. \quad (35)$$

This condition explains why it was legitimate to limit the range of  $s$  to 1 in the reminder formula.

### Appendix II - Liouville space formulation of quantum dynamics

Quantum dynamics is traditionally described in Hilbert space. However, it is convenient, in particular for open quantum systems, to introduce an extended space where density operators are vectors and time evolution is generated by a Schrödinger-like equation. This space is usually referred to as Liouville space [62]. We denote the "density vector" by  $|\rho\rangle \in \mathbb{C}^{1 \times N^2}$ . It is obtained by reshaping the density matrix  $\rho$  into a larger single vector with index  $\alpha \in \{1, 2, \dots, N^2\}$ . The one-to-one mapping of the two matrix indices into a single vector index  $\{i, j\} \rightarrow \alpha$  is arbitrary, but has to be used consistently. The vector  $|\rho\rangle$  is not normalized to unity in general. Its norm is equal to the purity,  $\mathcal{P} = \text{tr}(\rho^2) = \langle \rho | \rho \rangle$  where  $\langle \rho | = |\rho\rangle^\dagger$  as usual. The equation of motion of the density vector in

Liouville space follows from  $d_t \rho_\alpha = \sum_\beta \rho_\beta \partial(d_t \rho_\alpha) / \partial \rho_\beta$ . Using this equation, one can verify that the dynamics of the density vector  $|r\rangle$  is governed by a Schrödinger-like equation in the new space,

$$i \partial_t |\rho\rangle = \mathcal{H} |\rho\rangle, \quad (36)$$

where the super-Hamiltonian  $\mathcal{H}^{tot} \in \mathbb{C}^{N^2 \times N^2}$  is given by,

$$\mathcal{H}_{\alpha\beta} = i \frac{\partial(d_t \rho_\alpha)}{\partial \rho_\beta}. \quad (37)$$

A particularly useful index mapping is described in [72] and in [65]. For this form  $\mathcal{H}$  has a very simple form in terms of original Hilbert space Hamiltonian and Lindblad operators.

$\mathcal{H} = \mathcal{H}^H + \mathcal{L}$  is non-Hermitian for open quantum systems.  $\mathcal{H}^H$  originates from the Hilbert space Hamiltonian  $H$ , and  $\mathcal{L}$  from the Lindblad terms.  $\mathcal{H}^H$  is always Hermitian. The skew-Hermitian part  $(\mathcal{L} - \mathcal{L}^\dagger)/2$  is responsible for purity changes. Yet, in Liouville space, the Lindblad operators  $A_k$  (1) may also generate a Hermitian term  $(\mathcal{L} + \mathcal{L}^\dagger)/2$ . Though Hermitian in Liouville space this term cannot be associated with a Hamiltonian in Hilbert space.

For time-independent  $\mathcal{H}$  the evolution operator in Liouville space is:

$$|\rho(t)\rangle = \mathcal{K} |\rho(t')\rangle = e^{-i\mathcal{H}(t-t')} |\rho(t')\rangle. \quad (38)$$

If  $\mathcal{L} = 0$ ,  $\mathcal{K}$  is unitary. The fact that the evolution operator can be written as an exponent of a matrix, without any commutators as in Hilbert space, is a very significant advantage (see for example [68]). It is important to note that not all vectors in Liouville space can be populated exclusively. This is due to the fact that only positive  $\rho$  with unit trace are legitimate density matrices. The states that can be populated exclusively describe steady states, while others correspond to transient changes. We remind that in this paper we will use calligraphic letters to describe operators in Liouville space and ordinary letters for operators in Hilbert space. For states, however,  $|A\rangle$  will denote a vector in Liouville space formed from  $A_{N \times N}$  by “vec-ing”  $A$  into a column in the same procedure  $\rho$  is converted into  $|\rho\rangle$ .

### Useful relations in Liouville space.

In Liouville space, the standard inner product of two operators in Hilbert space  $\text{tr} A^\dagger B$  reads

$$\text{tr} A^\dagger B = \langle A | B \rangle.$$

In particular the purity  $\mathcal{P} = \langle r | r \rangle$  is just the square of the distance from the origin in Liouville space.

A useful relation for  $\mathcal{H}^H$  :

$$\mathcal{H}^H |H\rangle = \langle H | \mathcal{H}^H = 0. \quad (39)$$

The proof is as follows:

$$\mathcal{H}_{ij,mn}^H = H_{im} \delta_{jn} - H_{nj} \delta_{im}. \quad (40)$$

Therefore, using (40) we get:

$$\mathcal{H}^H |H\rangle = \sum_\beta \mathcal{H}_{\alpha\beta}^H H_\beta = \sum_{mn} \mathcal{H}_{ijmn}^H H_{mn} = [H, H] = 0 \quad (41)$$

This property is highly useful. We stress that (39) is a property of Hermitian operators in Hilbert space where both  $H$  and  $\mathcal{H}$  are well defined. A general Hermitian operator in Liouville space may not have a corresponding  $H$  in Hilbert space.

Another property that immediately follows from (40) is

$$\mathcal{H}_{ii,kk}^H = 0. \quad (42)$$

This corresponds to a well known property of unitary operation. If the system starts from a diagonal density matrix, then for short times the evolution generated by  $\mathcal{H}^H$ ,  $e^{-i\mathcal{H}^H dt} = I - i\mathcal{H}^H dt + O(dt^2)$  does not change the population in the leading order.

### Expectation values and their time evolution in Liouville space

The expectation value of an operator in Hilbert space is  $\langle A \rangle = \text{tr}(\rho A)$ . Since  $\rho$  is Hermitian the expectation value is equal to the inner product of  $A$  and  $\rho$  and therefore:

$$\langle A \rangle = \text{tr}(\rho A) = \langle \rho | A \rangle.$$

the dynamics of  $\langle A \rangle$  under Lindblad evolution operator:

$$\frac{d}{dt} \langle A \rangle = -i \langle A | \mathcal{H} | \rho \rangle + \left\langle \rho \left| \frac{d}{dt} A \right. \right\rangle. \quad (43)$$

Note that in Liouville space there is no commutator term since  $\mathcal{H}$  operates on  $|\rho\rangle$  just from the left. If the total Hamiltonian is Hermitian and time independent the conservation of energy follows immediately from applying (43) and (39) for  $A = H$ .

### Appendix III - The symmetric rearrangement theorem (SRT)

The goal of this Appendix is to explain why the equivalence of evolution operators leads to equivalence of work and equivalence of heat. In addition it is shown why it is valid also for transients. For the equivalence of evolution operator we have required that the super Hamiltonian is symmetric and that the action is small:

$$\mathcal{H}(t) = \mathcal{H}(-t), \quad (44)$$

$$s = \int_{-\tau/2}^{+\tau/2} \|\mathcal{H}\| dt \ll \hbar. \quad (45)$$

Let the initial state at time  $t = -\tau/2$  be

$$|\tilde{\rho}_i\rangle = |\tilde{\rho}(-\tau/2)\rangle. \quad (46)$$

this state leads to a final state at  $\tau/2$

$$|\tilde{\rho}_f\rangle = |\tilde{\rho}(\tau/2)\rangle. \quad (47)$$

Our goal is to evaluate a symmetric expectation value difference of the form:

$$\begin{aligned} dA_{tot} &= [\langle A(t_2) \rangle - \langle A(t_1) \rangle] + [\langle A(-t_1) \rangle - \langle A(-t_2) \rangle] \\ &= [\langle A | \tilde{\rho}(t_2) \rangle - \langle A | \tilde{\rho}(t_1) \rangle] \\ &\quad + [\langle A | \tilde{\rho}(-t_1) \rangle - \langle A | \tilde{\rho}(-t_2) \rangle], \end{aligned} \quad (48)$$

$$t_2, t_1 \geq 0$$

that is, the change in the expectation value of  $A$  in the segment  $[t_1, t_2]$  and its symmetric counterpart in negative time (e.g. the green areas in Fig. 11a). When  $A$  is equal to  $H_0$  this difference will translate into work or heat. We start with the expansion:

$$\begin{aligned} [\langle A(t_2) \rangle - \langle A(t_1) \rangle] &= \langle A | \mathcal{K}_{t_1 \rightarrow t_2} - I | \tilde{\rho}(t_1) \rangle = \\ &\left\langle A \left| -i\mathcal{H}(t_1)\delta t - \frac{1}{2}\mathcal{H}(t_1)^2\delta t^2 | \tilde{\rho}(t_1) \right\rangle + O(s^3). \end{aligned} \quad (49)$$

For the negative side we get:

$$\begin{aligned} [\langle A(-t_1) \rangle - \langle A(-t_2) \rangle] &= \langle A | I - \mathcal{K}_{-t_1 \rightarrow -t_2} | r(-t_1) \rangle = \\ &\left\langle A \left| -i\mathcal{H}(-t_1)\delta t + \frac{1}{2}\mathcal{H}(-t_1)^2\delta t^2 | \tilde{\rho}(-t_1) \right\rangle + O(s^3). \end{aligned} \quad (50)$$

Next we use the fact that:

$$|\tilde{\rho}(t_1)\rangle = |\tilde{\rho}(0)\rangle - i \int_0^{t_1} \mathcal{H}(t) dt |\tilde{\rho}(0)\rangle + O(s^2), \quad (51)$$

$$|\tilde{\rho}(-t_1)\rangle = |\tilde{\rho}(0)\rangle + i \int_0^{t_1} \mathcal{H}(t) dt |\tilde{\rho}(0)\rangle + O(s^2). \quad (52)$$

When adding the two segments the second order cancels out and we get:

$$\delta A_{tot} = -2i \langle A | \mathcal{H}(t_1) | \tilde{\rho}(0) \rangle \delta t + O(s^3). \quad (53)$$

Note that the result using  $|\tilde{\rho}(0)\rangle$  which is not given explicitly. To correctly relate it to  $|\tilde{\rho}(-\tau/2)\rangle$  we have to use symmetric rearrangement properties of the evolution operator.

### Symmetric rearrangement

In Fig. 11a there is an illustration of some time dependent Hamiltonian with reflection symmetry  $\mathcal{H}(t) =$

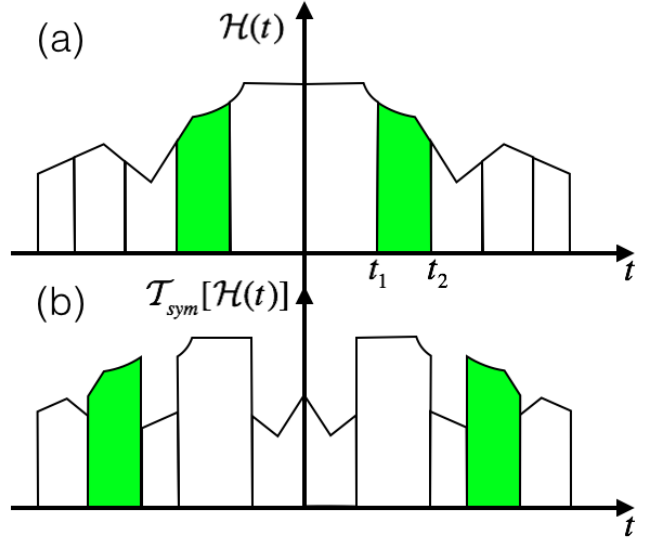


Figure 11: The Hamiltonians in (a) and (b) are related by symmetric rearrangement of the time segments. Up to a small correction  $O(s^3)$  the change in expectation values of an observable  $A$  that takes place during the green segments is the same in both cases. This effect explains why work and heat are the same in various types of engines when  $s$  is small compared to  $\hbar$  (equivalence regime).

$\mathcal{H}(-t)$ . We use  $\mathcal{H}$  to denote a Liouville space operator which may be any unitary operation or Markovian Lindblad operation. Assume that in addition to the symmetric bins of interest (green bins) the remainder of the time is also divided into bins in a symmetric way so that there is still a reflection symmetry also in the bin partitioning. Now, we permute the bins in the positive side as desired, and then make the opposite order in the negative side so that the reflection symmetry is kept. An example of such an operation is shown in Fig. 11b. Due to the Strang decomposition we know that the total evolution operator will stay the same under this rearrangement up to third order:

$$\mathcal{K}_{-\frac{\tau}{2} \rightarrow \frac{\tau}{2}} = \mathcal{T}_{sym}[\mathcal{K}]_{-\frac{\tau}{2} \rightarrow \frac{\tau}{2}} + O(s^3), \quad (54)$$

where  $\mathcal{T}_{sym}[x]$  stands for evaluation of  $x$  after a symmetric reordering.

### The symmetric rearrangement theorem (SRT)

From (54) we get that if the initial state is the same for a system described by  $\mathcal{K}$ , and for a system described by  $\mathcal{T}_{sym}[\mathcal{K}]$ , the final state at  $t = \tau/2$  is the same for both systems up to a third order correction:

$$\left| \tilde{\rho}\left(\frac{\tau}{2}\right) \right\rangle = \mathcal{T}_{sym}\left[\left| \tilde{\rho}\left(\frac{\tau}{2}\right) \right\rangle\right] + O(s^3). \quad (55)$$

Using (51),(52) we see that:

$$|\tilde{\rho}(0)\rangle = \frac{\left| \tilde{\rho}\left(\frac{\tau}{2}\right) \right\rangle + \left| \tilde{\rho}\left(-\frac{\tau}{2}\right) \right\rangle}{2} + O(s^2), \quad (56)$$

and because of (55) it also holds that:

$$\mathcal{T}_{sym}[|\tilde{\rho}(0)\rangle] = |\tilde{\rho}(0)\rangle + O(s^2) = \frac{|\tilde{\rho}(\frac{\tau}{2})\rangle + |\tilde{\rho}(-\frac{\tau}{2})\rangle}{2} + O(s^2), \quad (57)$$

using this in (53) we get that:

$$\delta A_{tot} = -2i \langle A | \mathcal{H}(t_1) \frac{|\tilde{\rho}(\frac{\tau}{2})\rangle + |\tilde{\rho}(-\frac{\tau}{2})\rangle}{2} \delta t + O(s^3). \quad (58)$$

Expression (58) no longer depends on the position of the time segment, but only on its duration and on the value of  $\mathcal{H}$ . Thus, the SRT states that the expression above also holds for any symmetric rearrangement

$$dA_{tot} = \mathcal{T}_{sym}[dA_{tot}] + O(s^3). \quad (59)$$

If we replace  $A$  by  $H_0$  and  $\mathcal{H}(t_1)$  by  $\mathcal{L}_c, \mathcal{L}_h$  or  $\mathcal{H}_w$  we immediately get the invariance of heat and work to symmetric rearrangement (up to  $s^3$ ). If  $|\tilde{\rho}(-\frac{\tau}{2})\rangle$  is the same for all engines then  $|\tilde{\rho}(\frac{\tau}{2})\rangle$  is also the same for all engines types up to  $O(s^3)$ . Consequently for all stroke engines the expression for work and heat are:

$$W = -2i \langle A | \int_{t \in t_w} \mathcal{H}_w(t) dt \frac{|\tilde{\rho}(\frac{\tau}{2})\rangle + |\tilde{\rho}(-\frac{\tau}{2})\rangle}{2} + O(s^3),$$

$$Q_{c(h)} = -2i \langle A | \int_{t \in t_{c(h)}} \mathcal{L}_{c(h)}(t) dt \frac{|\tilde{\rho}(\frac{\tau}{2})\rangle + |\tilde{\rho}(-\frac{\tau}{2})\rangle}{2} + O(s^3). \quad (60)$$

$$(61)$$

Using the identity  $|\tilde{\rho}(\frac{\tau}{2})\rangle + |\tilde{\rho}(-\frac{\tau}{2})\rangle = |\tilde{\rho}(t)\rangle + |\tilde{\rho}(-t)\rangle + O(s^2)$  that follows from (56), the integration over time of the energy flows  $j_w = \langle H_0 | \frac{1}{2} \mathcal{H}_w | \tilde{\rho}(t) \rangle$  and  $j_{c(h)} = \langle H_0 | \mathcal{L}_{c(h)} | \tilde{\rho}(t) \rangle$  for continuous engines, yields expressions (60) and (61) once more. This implies that the SRT (60) and (61) holds even if the different operations  $\mathcal{L}_c, \mathcal{L}_h$  and  $\mathcal{H}_w$  overlap with each other.

We emphasize that all the above relations hold for any initial state and not only in steady state where  $|\tilde{\rho}(\frac{\tau}{2})\rangle = |\tilde{\rho}(-\frac{\tau}{2})\rangle$ . The physical implication is that in the equivalence regime different engines are thermodynamically indistinguishable when monitored at the end of each cycle, even when the system is not in its steady state.

- 
- [1] F. Curzon and B. Ahlborn, Am. J. Phys. **43**, 22 (1975).
  - [2] I. Novikov, Journal of Nuclear Energy **7**, 125 (1958).
  - [3] P. Salamon, J.D. Nulton, G. Siragusa, T.R. Andersen and A. Limon, Energy **26**, 307 (2001).
  - [4] B. Andresen, Angewandte Chemie International Edition **50**, 2690 (2011).
  - [5] R. Alicki, J. Phys A: Math.Gen. **12**, L103 (1979).
  - [6] R. Kosloff, J. Chem. Phys. **80**, 1625 (1984).
  - [7] E. Geva and R. Kosloff, J. Chem. Phys. **96**, 3054 (1992).
  - [8] T. Feldmann and R. Kosloff, Phys. Rev. E **61**, 4774 (2000).
  - [9] Y. Rezek and R. Kosloff, New J. Phys. **8**, 83 (2006).
  - [10] R. Kosloff and A. Levy, Annual Review of Physical Chemistry **65**, 365 (2014).
  - [11] U. Harbola, S. Rahav, and S. Mukamel, Euro. Phys. Lett. **99**, 50005 (2012).
  - [12] A. E. Allahverdyan, K. Hovhannisyanyan, and G. Mahler, Phys. Rev. E **81**, 051129 (2010).
  - [13] N. Linden, S. Popescu, and P. Skrzypczyk, Phys. Rev. Lett. **105**, 130401 (2010).
  - [14] A. L. Correa, P. J. Palao, D. Alonso, and G. Adesso, Phys. Rev. E **87**, 042123 (2013).
  - [15] M. J. Henrich, F. Rempp, G. Mahler, Eur. Phys. J. **151**, 157 (2005).
  - [16] P. Skrzypczyk, A. J. Short, and S. Popescu, Nature communications **5** (2014).
  - [17] D. Gelbwaser-Klimovsky, R. Alicki, and G. Kurizki, EPL (Europhysics Letters) **103**, 60005 (2013).
  - [18] M. Kolář, D. Gelbwaser-Klimovsky, R. Alicki, and G. Kurizki, Phys. Rev. Lett. **109**, 090601 (2012).
  - [19] R. Alicki, Open Systems & Information Dynamics **21** (2014).
  - [20] H. Quan, Y. x. Liu, C. Sun, and F. Nori, Physical Review E **76**, 031105 (2007).
  - [21] J. Roßnagel, O. Abah, F. Schmidt-Kaler, K. Singer, and E. Lutz, Phys. Rev. Lett. **112**, 030602 (2014).
  - [22] R. Dorner, S. Clark, L. Heaney, R. Fazio, J. Goold, and V. Vedral, Phys. Rev. Lett. **110**, 230601 (2013).
  - [23] R. Dorner, J. Goold, C. Cormick, M. Paternostro, and V. Vedral, Phys. Rev. Lett. **109**, 160601 (2012).
  - [24] F. Binder, S. Vinjanampathy, K. Modi, and J. Goold, arXiv preprint arXiv:1406.2801 (2014).
  - [25] A. del Campo, J. Goold, and M. Paternostro, Scientific reports **4** (2014).
  - [26] D. Gelbwaser-Klimovsky, W. Niedenzu, and G. Kurizki, arXiv preprint arXiv:1503.01195 (2015).
  - [27] A. S. Malabarba, A. J. Short, and P. Kammerlander, arXiv preprint arXiv:1412.1338 (2014).
  - [28] M. Horodecki and J. Oppenheim, Nature communications **4** (2013).
  - [29] Lidia del Rio, Johan Aberg, Renato Renner, Oscar Dahlsten and Vlatko Vedral, Nature **474**, 61 (2011).
  - [30] J. Gemmer, M. Michel and G. Mahler, *Quantum Thermodynamics* (Springer, 2009).
  - [31] A. Riera, C. Gogolin, and J. Eisert, Phys. Rev. Lett. **108**, 080402 (2012).
  - [32] S. Trotzky, Y.-A. Chen, A. Flesch, I. P. McCulloch, U. Schollwöck, J. Eisert, and I. Bloch, Nature Physics **8**, 325 (2012).
  - [33] H. Spohn, Journal of Mathematical Physics **19**, 1227 (1978).
  - [34] M. Campisi, P. Talkner, and P. Hänggi, Phys. Rev. Lett. **102**, 210401 (2009).
  - [35] M. Campisi, P. Hänggi, and P. Talkner, Rev. Mod. Phys.



- 83**, 771 (2011).
- [36] H. Quan and H. Dong, arXiv preprint arXiv:0812.4955 (2008).
- [37] M. Lostaglio, K. Korzekwa, D. Jennings, and T. Rudolph, Phys. Rev. X **5**, 021001 (2015), URL <http://link.aps.org/doi/10.1103/PhysRevX.5.021001>.
- [38] M. Lostaglio, D. Jennings, and T. Rudolph, Nature communications **6** (2015).
- [39] S. Rahav, U. Harbola, and S. Mukamel, Phys. Rev. A **86**, 043843 (2012).
- [40] M. O. Scully, M. S. Zubairy, G. S. Agarwal, H. Walther, Science **299**, 862 (2003).
- [41] M. O. Scully, K. R. Chapin, K. E. Dorfman, M. B. Kim, and A. Svidzinsky, Proceedings of the National Academy of Sciences **108**, 15097 (2011).
- [42] R. Alicki and M. Fannes, Phys. Rev. E **87**, 042123 (2013).
- [43] K. V. Hovhannisyanyan, M. Perarnau-Llobet, M. Huber, and A. Acín, Phys. Rev. Lett. **111**, 240401 (2013).
- [44] G. Gennaro, G. Benenti, and G. M. Palma, EPL (Europhysics Letters) **82**, 20006 (2008).
- [45] G. Gennaro, G. Benenti, and G. M. Palma, Phys. Rev. A **79**, 022105 (2009).
- [46] T. Rybár, S. N. Filippov, M. Ziman, and V. Bužek, Journal of Physics B: Atomic, Molecular and Optical Physics **45**, 154006 (2012).
- [47] M. Ziman, P. Štelmachovič, and V. Bužek, Open Systems & Information Dynamics **12**, 81 (2005).
- [48] R. Uzdin and R. Kosloff, New Journal of Physics **16**, 095003 (2014).
- [49] M. Esposito, K. Lindenberg, and C. Van den Broeck, Phys. Rev. Lett. **102**, 130602 (2009).
- [50] R. Kosloff, Entropy **15** (2013).
- [51] J. Anders and V. Giovannetti, New Journal of Physics **15**, 033022 (2013).
- [52] Ronnie Kosloff and Tova Feldmann, Phys. Rev. E **82**, 011134 (2010).
- [53] M. Campisi, J. Phys A: Math.theor. **47**, 245001 (2014).
- [54] A. E. Allahverdyan, K. Hovhannisyanyan, and G. Mahler, Phys. Rev. E **81**, 051129 (2010).
- [55] H. E. D. Scovil and E. O. Schulz-DuBois, Phys. Rev. Lett. **2**, 262 (1959).
- [56] E. Geva and R. Kosloff, J. Chem. Phys. **104**, 7681 (1996).
- [57] A. Levy and R. Kosloff, Euro. Phys. Lett. **107**, 20004 (2014).
- [58] H.-P. Breuer and F. Petruccione, *Open quantum systems* (Oxford university press, 2002).
- [59] G. Lindblad, J. Phys A: Math.Gen. **48**, 119 (1976).
- [60] V. Gorini, A. Kossakowski and E.C.G. Sudarshan, J. Math. Phys. **17**, 821 (1976).
- [61] E. Davies, Commun. Math. Phys. **39**, 91 (1974).
- [62] S. Mukamel, *Principles of nonlinear optical spectroscopy*, vol. 29 (Oxford University Press New York, 1995).
- [63] A. Rivas, A.D.K. Plato, S.F. Huelga and M.B. Plenio, New Journal of Physics **12**, 11303 (2010).
- [64] T. Jahnke and C. Lubich, BIT Numerical Mathematics **40**, 735 (2000).
- [65] H. Roger and R. J. Charles, *Topics in matrix analysis* (Cambridge University Press, 1994).
- [66] A. E. Allahverdyan, R. Balian, and Th. M. Nieuwenhuizen, Euro. Phys. Lett. **67**, 565 (2004).
- [67] Tova Feldmann and Ronnie Kosloff, Phys. Rev. E **73**, 025107(R) (2006).
- [68] Uzdin, Raam and Lutz, Eric and Kosloff, Ronnie, arXiv:1408.1227 (2014).
- [69] R. Uzdin, U. Günther, S. Rahav, and N. Moiseyev, Journal of Physics A: Mathematical and Theoretical **45**, 415304 (2012).
- [70] R. Uzdin and O. Gat, Physical Review A **88**, 052327 (2013).
- [71] R. Uzdin, Journal of Physics A: Mathematical and Theoretical **46**, 145302 (2013).
- [72] Machnes, Shai and Penio, Martin B., arXiv:1408.3056v1 (2014).
- [73] other types consist of small variations and combination of these types.
- [74] This is, of course, not true for the work repository.
- [75] This can be seen by following the derivation in [58] and using formalism introduced in [72].
- [76] because of the property  $\langle H_0 | \mathcal{H}_0 = 0$ ,  $\langle H_0 |$  is not modified by the transformation to the interaction picture.
- [77] Note that since  $\mathcal{K} = e^{-i\mathcal{H}_0\tau_{cyc}}\tilde{\mathcal{K}}$ , the equivalence of the evolution operators holds also in the original frame not just in the interaction frame.
- [78] For simplicity we think of a single particle engine. Thus entanglement and spin statistics are irrelevant quantum effects. In addition, in the weak system-bath coupling limit the entanglement to the baths is negligible.
- [79] This is very well known in the context of the Zeno effect.
- [80] In the Lindblad framework any thermalization is intrinsically associated with some dephasing. Yet, here we assume an additional controllable dephasing mechanism.